Structure and magnetism of multiphase $Sm_{0.080}Co_{0.645}Fe_{0.276}$ powders

V. G. Harris, M. Liou,[a] B. N. Das, V. M. Browning, J. E. Snyder, M. Rubinstein, and S. H. Lawrence
U.S. Naval Research Laboratory, Washington, DC 20375-5000

R. Littleton III[b] and D. P. Pappas
Virginia Commonwealth University, Richmond, Virginia 23284-2000

A Sm-poor mixture of Fe-substituted Sm_2Co_{17}, having the nominal stoichiometry of $Sm_{0.080}Co_{0.645}Fe_{0.276}$, was ball-milled to explore the possibility of enhancing its remanence through direct microstructural refinement. With milling, the $Sm_2(Co_{0.7}Fe_{0.3})_{17}$ compound disassociates to a body-centered-cubic supersaturated SmCoFe solid solution and a residual SmCoFe amorphous phase. Correspondingly, the coercive field values first increase, peaking at 0.83 kOe after 180 min of milling, then decrease with continued milling to <0.1 kOe after 1200 min. The remanence, as M_r/M_s, is measured to track closely the coercive field behavior, experiencing modest increases to 0.26 after just 120 min of milling. Magnetization values are found to increase first with the dissociation of the 2:17 phase, and again with the ejection of Sm from the bcc component. © *1997 American Institute of Physics.* [S0021-8979(97)20608-0]

As reported by Coey in a recent perspective on permanent magnetism,[1] exchange coupled nanostructures offer a unique path toward developing isotropic coercive powders with remanence values exceeding the $M_s/2$ limit applicable to noninteracting isotropically aligned crystallites. This mechanism has been shown to exist in both single phase[2,3] and two phase[4–7] systems. In the two phase systems, the focus of this paper, hard magnet crystallites are exchange coupled to soft magnet crystallites having an approximate length scale twice that of the domain wall width of the hard phase.[8,9] Most examples of these systems involve $Nd_2Fe_{14}B$ as the hard phase with either Fe or Fe_3B as the soft phase.[4–6] An exception is the work of Ding *et al.*[7] and O'Donnell *et al.*,[10] who both employed ball-milling to Sm-poor mixtures of SmFe, followed by anneals under flowing N_2 gas, to produce Sm–Fe–N exchange coupled nanostructures.

In this paper, we employ ball-milling of a Sm-poor mixture of SmCoFe to explore the possibility of directly enhancing the remanence via the mechanical attrition of an appropriately chosen mixture.

Powder samples having the nominal stoichiometry of $Sm_{0.080}Co_{0.645}Fe_{0.276}$ were ball-milled in a Spex™ mill for times ranging from 60 to 1200 min. Starting materials for the milling operation were a $Sm_2(Co_{0.7}Fe_{0.3})_{17}$ ingot and elemental Co and Fe powders at a ratio of 7:3, leading to a 3:1 ratio between the 2:17 compound and metallic CoFe, i.e., $[Sm_2(Co_{0.7}Fe_{0.3})_{17}]_{0.75}[Co_{0.7}Fe_{0.3}]_{0.25}$. The $Sm_2(Co_{0.7}Fe_{0.3})_{17}$ compound was processed by arc-melting the elemental constituents on a water cooled Cu hearth under a positive pressure of gettered Ar gas. After arc melting the ingot was pulverized in a hardened steel mortar and pestle and introduced to the Spex™ mill, with additives of elemental Co and Fe powders. The cylinder was sealed in an Ar gas environment to retard oxidation of the powder during milling. Four hardened steel balls, two having radii of 6 mm and two having radii of 3 mm, were used in the milling operation. At predetermined times the milling was suspended and a sample of the powder was extracted for superconducting quantum interference device (SQUID) magnetometry, x-ray diffraction (XRD), and extended x-ray absorption fine structure (EXAFS).[11]

SQUID measurements were performed on powder samples by confining the powder within a thin walled Ta tube (1.5 mm diam) which in turn was constrained in an evacuated quartz ampoule. Hysteresis loops of the powder samples were collected using a maximum applied field of 4 T. X-ray diffraction θ–2θ diffraction scans were performed using K_α radiation from a fixed anode Cu source. Lattice parameters (a_0) of the bcc phase were calculated using d-spacings measured from three or more diffraction lines and plotted against the Nelson–Riley equation.[12]

A summary of the XRD and SQUID measurements for the ball-milled $Sm_{0.080}Co_{0.645}Fe_{0.276}$ samples are presented in Figs. 1, 2, and 3. Figure 1 is a plot of portions of θ–2θ XRD scans vertically offset from one another, but all sharing a common x-axis and the same y-axis subscale, to allow a meaningful comparison of peak amplitudes between plots. In the early stages of milling, i.e, 60 min$\leqslant t \leqslant$300 min, one sees that the peak amplitudes experience a reduction in amplitude with increasing widths. These trends are common in ball-mill processing and are caused by a reduction of crystallite size with increased milling time. However, also evident over this time interval is the preferential reduction in the amplitude of the 2:17 peaks compared with the bcc peaks. This is most clearly depicted in Fig. 2(a) where the amplitudes of the (220) peak of the 2:17 phase and the (110) peak of the bcc phase are plotted together versus milling time. Figure 2(b) is a plot of the half-width at half-maximum (HWHM) values for these same peaks. The HWHM is used here qualitatively to monitor crystallite size as a function of milling time: the HWHM is inversely proportional to the crystallite size. In this plot one sees that the HWHM values for the 2:17 phase increase exponentially with milling time while the values for the bcc component increase, but not as much and at a much slower rate. The likely reason for this behavior is the brittle nature of the 2:17 component, relative to the bcc solution, allows the faster reduction in particle size. As can be seen in

[a]Present address: School of Engineering, Cornell University, Ithaca, New York.
[b]Present address: Department of Physics, Clemson University, Clemson, South Carolina.

 0021-8979/97/81(8)/5121/3/$10.00

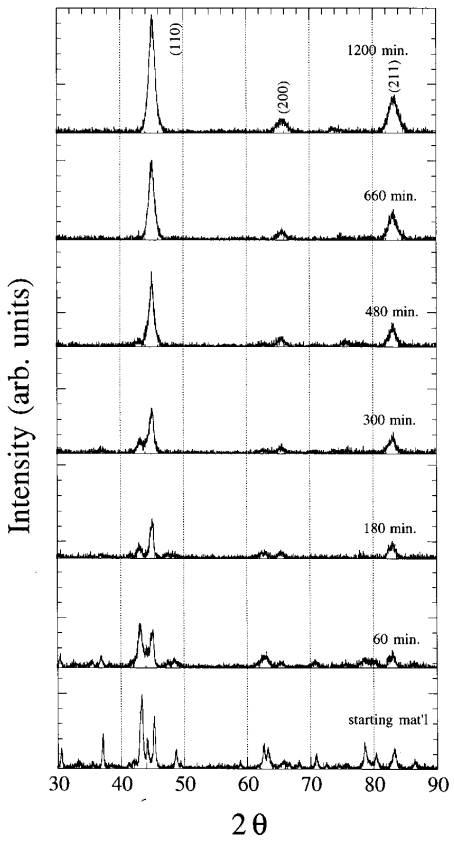

FIG. 1. Regions of the θ–2θ x-ray diffraction scans for samples milled at various times. Plots are vertically offset from one another but share a common x-axis and the same y-axis subscale to allow the meaningful comparison of the peak positions and amplitudes between plots.

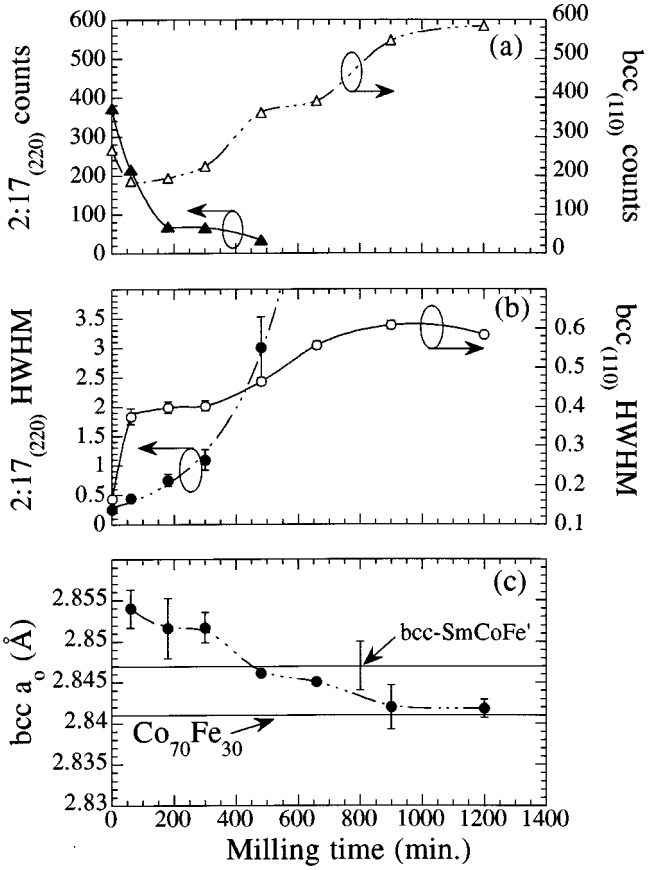

FIG. 2. (a) Diffraction peak amplitudes for the $bcc_{(110)}$ and the $2{:}17_{(220)}$ peaks; (b) HWHM values from the $bcc_{(110)}$ and the $2{:}17_{(220)}$ peaks; and (c) the lattice parameter, a_0, for the bcc component as a function of ball-milling time.

Fig. 1, and inferred from Figs. 2(a) and 2(b), after 600 min of milling the 2:17 diffraction features are no longer visible, while the bcc features, although broader, have much larger amplitudes. The significant increase in both HWHM and the peak amplitudes for the bcc peaks can only be explained by the disassociation of the 2:17 compound, in part, to a bcc phase. The milling was continued for 1200 min whereupon only broad bcc diffraction peaks were detected.

The lattice parameter a_0 of the bcc component was measured as a function of milling time and is plotted in Fig. 2(c). Here one sees that the a_0 values are largest at low milling times. This can be attributed to the presence of elemental bcc Fe as a starting material: The lattice parameter of bcc Fe is large, 2.867 Å, compared to that of the bcc CoFe alloy, 2.842 Å, which results from the milling of Co and Fe. As can be seen in Fig. 2(c), a_0 of the bcc component decreases with milling time. After 480 and 660 min of milling the bcc a_0 values are approximately equal to the value measured for the bcc SmCoFe′ phase in the arc-melted $Sm_{0.105}Co_{0.626}Fe_{0.268}$ ingot. With continued milling, 660 min$\leqslant t \leqslant$1200 min, these values gradually reduce to approximately that of the bcc CoFe alloy.

Figures 3(a)–3(c) are plots of the magnetization, coercivity and remanence, as M_r/M_s, respectively. The magnetization of the samples is measured to experience two distinct transitions with milling time. The first transition is detected as an increase in magnetization occurring immediately after milling commences, and tracks closely with the reduction in the 2:17 peak amplitudes. The increase in magnetization over this range is due to the conversion of the 2:17 compound to the more magnetic SmCoFe bcc and amorphous SmCoFe phases. The rate of increase in the magnetization values slows over 180 min$\leqslant t \leqslant$480 min coinciding with the elimination of the 2:17 phase. A second transition, beginning at t=480 min and extending to t=1200 min, signals another large increase in magnetization. This increase is due to the expulsion of Sm from the SmCoFe solid solution to a high-spin bcc CoFe solution.

The coercivity of the powder samples was measured to first increase sharply then decrease as a function of milling time [Fig. 3(b)]. The initial increase is attributed to an increase in the density of domain wall pinning centers in the form of lattice defects and grain boundaries caused by the milling process. The decrease with increased milling time comes from the softening of the hard component when it disassociates to the soft SmCoFe bcc and amorphous phases. The abrupt decrease, starting at $t \geqslant 180$ min, is spurred by the reduction of 2:17 particles below their paramagnetic limit. A plateau in the coercive field values, seen in Fig. 3(b) after 480 min of milling, which is also prominent in the M_r/M_s plot in Fig. 3(c), indicates that the Sm containing bcc phase has a higher intrinsic coercive field than the bcc CoFe alloy:

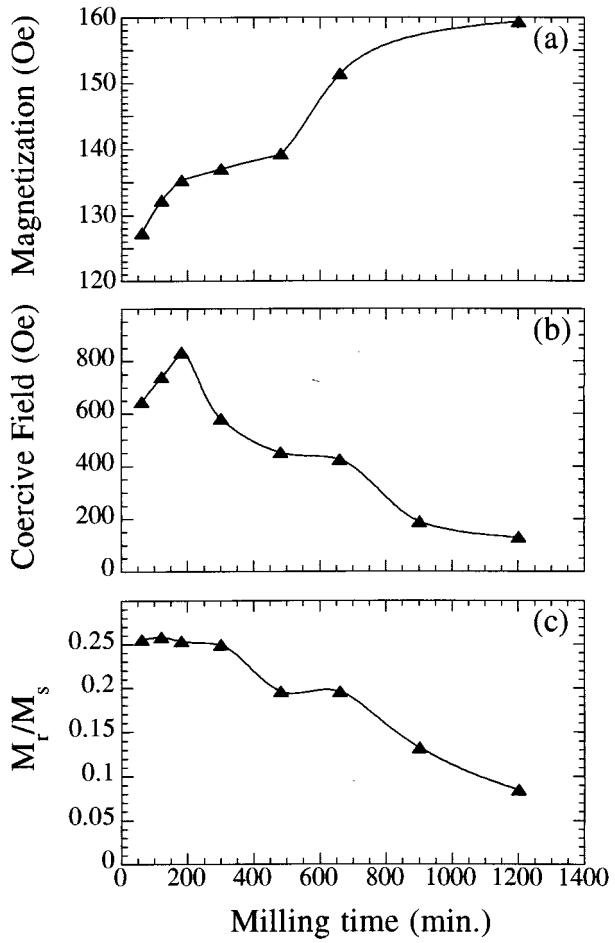

FIG. 3. (a) Magnetization, (b) coercive field, and (c) remanence (M_r/M_s) extracted from hysteresis loops collected from SQUID measurements as a function of milling time.

It is over this time frame that the Sm starts to be expelled from the SmCoFe solid solution. As expected, the anisotropy field values (not shown) track closely the coercive field values. However, they are much higher than expected for a soft CoFe alloy. This suggests that a significant amount of the Sm remains in the bcc phase even after long periods of ball-milling.

Presented in Table I is a summary of the structural evolution of the $Sm_{0.080}Co_{0.645}Fe_{0.276}$ mixture which occurs as a result of ball-milling. We define the structural evolution to occur in three stages: (I) the formation of a nanostructured mixture consisting of the original 2:17 and bcc SmCoFe (designated: SmCoFe′) phases, together with the newly alloyed elemental Co and Fe; and (II) the disassociation of the 2:17 component to a second bcc SmCoFe phase (designated: bcc SmCoFe″) and an amorphous SmCoFe phase (designated: *a*-SmCoFe). Continued milling facilitates a third transition where Sm is expelled from the SmCoFe bcc phases and results in a bcc CoFe solid solution and a residual amorphous phase.

Measurements of the Sm L_{III}, Fe *K* and Co *K* absorption edge EXAFS, for samples milled for several hours, indicate that the Fe and Co exist principly in a bcc phase, while the

TABLE I. Effect of ball-milling on the $Sm_{0.080}Co_{0.645}Fe_{0.276}$ mixture.

(S): $[Sm_2(Co_{0.7}Fe_{0.3})_{17}$+bcc SmCoFe′]+bcc Fe+hcp Co—BM→
(I): *n* $Sm_2(Co_{0.7}Fe_{0.3})_{17}$+ *n* bcc SmCoFe′+bcc CoFe— BM→
(II): *n* $Sm_2(Co_{0.7}Fe_{0.3})_{17}$+ *n* bcc SmCoFe′
+{bcc SmCoFe″+ *a* SmCoFe}+bcc CoFe—BM→
(III): *a* SmCoFe+bcc CoFe+Sm*

Notes: [ ]: indicates the phases present in the arc-melted charge used as a starting material.
(I,II,III): indicates the different stages of structural and chemical evolution.
S: starting mixture.
{ }: indicates disassociation products of the 2:17 phase.
BM: ball milling.
n: nanostructure.
a: amorphous.
*: In the late stages of milling we detected a Sm_2O_3 phase which likely formed from the elemental Sm (see the text).

Sm atoms exists in a multiple of sites, including Sm_2O_3 and an amorphous phase.[11] The presence of the Sm oxide is likely the result of the pure Sm expelled from the bcc crystallites which oxidizes on the crystallite surface. These results are consistent with previous studies that have shown ball-milling elemental equivalents of 2:17 lead to a two phase mixture of the transition metal and a Sm enriched amorphous phase.[7]

The disassociation of the 2:17 compound via mechanical attrition precludes the formation of an exchange coupled heterogeneous nanostructure. The brittle 2:17 crystallites are reduced in size below their superparamagnetic limit, prior to their disassociation, while the soft phase crystallite remains too large for effective exchange coupling. However, this system is still a favorable candidate to form an exchange coupled heterogeneous magnetic if it can be annealed to form a nanostructure having the appropriate length scales. Such an effort is currently underway.

During the course of this research M. Liou was supported by the George Washington University—Department of Defense Science and Engineering Apprenticeship Program, and J. E. Snyder was supported as a National Research Council—Naval Research Laboratory Research Associate. This research was supported, in part, by the Grant No. 96Pr03042-00 from the Office of Naval Research.

[1] J. M. D. Coey, J. Magn. Magn. Mater. **140–144**, 1041 (1995).
[2] R. W. McCallum, A. M. Kadin, G. B. Clemente, and J. E. Keem, J. Appl. Phys. **61**, 3577 (1987).
[3] H. A. Davies, A. Manaf, and P. Z. Zhang, J. Mater. Eng. Perf. **2**, 579 (1993).
[4] R. C. Coehoorn, D. B. d. Mooij, and C. de Waard, J. Magn. Magn. Mater. **80**, 101 (1989).
[5] S. Hirosawa, H. Kanekiyo, and M. Uehara, J. Appl. Phys. **73**, 6488 (1993).
[6] A. Manaf, R. A. Buckley, and H. A. Davies, J. Magn. Magn. Mater. **128**, 302 (1993).
[7] J. Ding, P. G. McCormack, and R. Street, J. Magn. Magn. Mater. **124**, L1 (1993).
[8] H. Fukunaga and H. Inoue, Jpn. J. Appl. Phys. **31**, 1347 (1992).
[9] T. Schrefl and J. Fidler, J. Appl. Phys. **79**, 6458 (1996).
[10] K. O'Donnell, X. L. Rao, G. Laird, and J. M. D. Coey, Phys. Status Solidi A **153**, 223 (1996).
[11] V. G. Harris (unpublished).
[12] J. B. Nelson and D. P. Riley, Proc. Phys. Soc. London **57**, 160 (1945).